



Supporting Online Material for  
**Coupled  $^{142}\text{Nd}$ - $^{143}\text{Nd}$  Isotopic Evidence for Hadean Mantle Dynamics**

**Vickie C. Bennett,\* Alan D. Brandon, Allen P. Nutman**

\*To whom correspondence should be addressed. E-mail: vickie.bennett@anu.edu.au

Published 21 December 2007, *Science* **318**, 1907 (2007)  
DOI: 10.1126/science.1145928

**This PDF file includes:**

Materials and Methods

Figs. S1 to S3

Tables S1 to S3

References

## **Supporting Online Material:**

### **Materials and Methods**

#### **Sample selection.**

All samples were collected by either Nutman or Bennett as part of an integrated fieldwork, geochronologic and geochemical program of investigation of Archean terranes at the Australian National University. Only samples collected from lower strain areas and that on the basis of rock textures, chemistry and U-Pb age characteristics of the zircon population were considered to be single phase orthogneisses and with no apparent secondary alteration were analysed. Mafic samples are either from a pillow basalt sequence in the western part of the Isua supracrustal belt, or homogeneous rocks from mafic-ultramafic sequences from islands in the vicinity of Nuuk. The ages of all granitic (*sensu lato*) samples were determined directly by in situ U-Pb dating of zircons using one of the Sensitive High Resolution Ion MicroProbes (SHRIMPs) at the Australian National University. The ages of mafic samples are constrained by U-Pb zircon ages of cross-cutting rocks and are thus minima. A summary of age information and references to published chemistry and locality information for each sample is provided in Table S1.

#### **Sample preparation.**

Fresh interior rock material was collected in the field using sledgehammers. The whole rock powders were processed by breaking 1-2 kg of fresh rock into less than 1 cm pieces. An aliquot of the rock chips was then powdered in an Al<sub>2</sub>O<sub>3</sub> or tungsten carbide mill. <sup>147</sup>Sm-<sup>143</sup>Nd compositions were determined at the Australian National University (ANU), with data for some samples previously published (Tables S1 and S2). The techniques in use at the ANU have been reported elsewhere (*e.g. S1*) and are summarised here. 100-200mg sample powder aliquots were weighed into Teflon pressure digestion containers along with a mixed <sup>147</sup>Sm-<sup>150</sup>Nd isotope spike originally calibrated against a California Institute of Technology mixed Sm-Nd concentration standard. Distilled HF-HCl-HNO<sub>3</sub> acids were added and digestion vessels placed on hotplate at 180°C overnight. After gentle drying, fresh HF and HNO<sub>3</sub> acids were added and the teflon container was encased in a steel jacket (Parr bomb) and placed in a 200 °C oven for >48 hours. This high-pressure step is considered essential for Archean samples in order to achieve complete sample dissolution and spike equilibration for both felsic and mafic samples. After cooling the samples were taken to dryness on a hot plate and brought back into solution in 1.0N HCl. The

centrifuged samples solutions were loaded onto cation columns to separate REE from the rock matrix. Final separation of Sm and Nd was achieved using an HDEHP column.

The high precision  $^{142}\text{Nd}$  isotopic measurements were made at the Johnson Space Center Labs on separate powder aliquots. A similar procedure digestion procedure, but without spike addition was followed. For felsic rocks the high pressure dissolution step was included; mafic samples were dissolved on a hot plate in closed Teflon beakers. Complete sample dissolution is not a concern for accurate  $^{142}\text{Nd}$  isotopic determinations as no correction for in situ decay is necessary for rocks of this age. After dissolution the REE were separated from the rock matrix either using conventional cation exchange columns or Eichrom Tru-Spec resin using 100ul polypropylene columns. The REE fractions then loaded on Eichrom Ln-spec resin columns to isolate Nd from rest of the REE fraction. A significant problem with determining  $^{142}\text{Nd}$  compositions is the elimination of Ce and more specifically the isobaric interference from  $^{142}\text{Ce}$ . To quantitatively remove the Ce, the Nd cut was further purified using a solvent extraction method (S2). Cerium was first oxidized in a solution of  $\text{NaBrO}_3$  and 10 M  $\text{HNO}_3$  to take advantage of the preferential partitioning of  $\text{Ce}^{4+}$  into organic solvent. The organic solvent consists of 3M HDEHP in n-heptane. The organic solvent was added to the solution containing  $\text{REE}^{3+}$  and oxidized  $\text{Ce}^{4+}$  resulting in Ce extraction into the solvent. After shaking and centrifuging, the organic solvent was discarded and the procedure was repeated three times. The solution was then purified for remaining traces of dissolved HDEHP and complexed  $\text{Ce}^{4+}$  by twice adding and then discarding pure n-heptane. Sodium from the  $\text{NaBrO}_3$  was eliminated from the Nd cuts using a small cation column of AG50-X8 resin. The Nd cut was purified one more time on the LN-Spec column. This procedure eliminates > 99.999% of Ce in the purified Nd cuts. Total procedural blanks are  $\leq 80$  pg and  $\leq 30$  pg for Nd and Sm, respectively. Chemistry yields are >80% for Nd and >95% for Sm.

### **Mass Spectrometry**

For Sm concentration determinations and Nd concentration and  $^{143}\text{Nd}/^{144}\text{Nd}$  isotopic measurements the Sm and Nd fractions were loaded separately onto Ta filaments as part of a double Ta-Re filament assembly and analysed as metals. Isotopic compositions were measured on either the ANU Finnigan Mat 261 or Triton thermal ionisation mass spectrometer in static

multi-collection mode. Data were reduced with an iterative spike subtraction, exponential fractionation correction algorithm and were corrected for fractionation using a value of  $^{146}\text{Nd}/^{144}\text{Nd}=0.7219$  and to a composition of the La Jolla standard  $=0.511860$ . Sm was monitored and not detected during the Nd analyses; Nd was monitored at mass 146 during Sm runs and was negligible. Owing to the high precision of Sm and Nd isotopic measurements, the errors in the calculated initial  $\epsilon^{143}\text{Nd}$  are due largely to uncertainties in spike calibration propagated over the age of the rocks and calculated to be  $\leq 0.5$  epsilon units for these early Archean samples.

For determination of high precision  $^{142}\text{Nd}/^{144}\text{Nd}$  isotopic ratios, approximately 600ng of Nd was loaded in  $\text{H}_3\text{PO}_4$  onto one filament of a previously outgassed double Re filament assembly. The isotope measurements were performed on the Triton TIMS at the Johnson Space Center with the source magnets removed (S3). Nd isotopes were measured as positive metal ions with the data normalized to  $^{146}\text{Nd}/^{144}\text{Nd} = 0.7219$  to correct for instrument mass fractionation during the runs. We used a three-line multi-dynamic data collection scheme, with amplifier rotation adapted from Caro et al. (S3). Zoom optics were used to center the masses in the cups after each peak jump. The focus parameters for each filament were kept within a narrow range with invariant Z focus, and for each sample the peak overlap and peak shapes for each of the three lines were examined prior to data collection. An analysis consisted of 180-360 blocks of data with each block consisting of 1 scan each through the 3 cup configuration, each of 16 seconds data integration. Typical  $^{142}\text{Nd}$  beam intensities were 5V, using a  $10^{11}$  ohm resistor, with data taken with a minimum beam size of 3V and a maximum of 7V  $^{142}\text{Nd}$ . The runs were typically 4-8 hours. Cerium was monitored throughout using  $^{140}\text{Ce}$  and on-line corrections were made. Samarium interferences were monitored using mass 147, which was never found to detectable on the faraday cups above baseline.

Standard runs were interspersed with sample runs. The samples were run in a random order and not by age or locality. During the course of this study 13 interspersed analyses of an AMES Nd standard solution (600ng loads) gave an average composition of  $^{142}\text{Nd}/^{144}\text{Nd}=1.1418385\pm 0.0000040$  yielding a  $2\sigma$  external reproducibility of  $\pm 3.5$  ppm (Table S3, figure S1). It is this average that is used as the terrestrial reference value for  $^{142}\text{Nd}/^{144}\text{Nd}$  for calculating  $^{142}\text{Nd}$  variations for the samples. Internal precisions ( $2\sigma/\sqrt{n}$ , with  $n$ =number of measurement cycles), for both samples and standards were typically  $\pm 2-3$  ppm, with complete

isotopic ratio data for standards and samples in Table S3. With multidynamic data collection the  $^{148}/^{144}$  ratio was measured in only 2 of the 3 scans and the  $^{150}/^{144}$  ratio was measured in 1 of the 3 scans resulting in commensurately poorer reproducibility for these ratios. In the following 3 months after completion of this work additional high precision  $^{142}\text{Nd}/^{144}\text{Nd}$  measurements of the AMES standard were made using identical methods. The average  $^{142}\text{Nd}/^{144}\text{Nd}$  for the additional 10 analyses was only 1.1 ppm different than the first standard set and with a slightly better external reproducibility of  $\pm 3$  ppm. The combined dataset of 23 AMES standards acquired over a 6 month period has an average composition of  $^{142}\text{Nd}/^{144}\text{Nd} = 1.1418390 \pm 0.0000034$  with  $2\sigma$  external reproducibility of  $\pm 3.3$  ppm, attesting to the long term stability of the JSC Triton in this measurement configuration. In addition measurement of Nd separated from 14 different modern rocks demonstrates an external reproducibility of  $^{142}\text{Nd}/^{144}\text{Nd}$  for chemically processed samples of  $\pm 3.4$  ( $2\sigma$ , Fig. S2)

As a further check of the accuracy and precision of the  $^{142}\text{Nd}/^{144}\text{Nd}$  measurements, a series of precise gravimetrically prepared  $^{142}\text{Nd}$  - enriched standards were measured with  $^{142}\text{Nd}/^{144}\text{Nd}$  excesses of 21.8 ppm, 43.0 ppm and 63.8 ppm compared with the AMES standard. The results of these analyses (Table S3) demonstrate that these measurements are accurately reproducible within  $\pm 3$  ppm over a wide range of  $^{142}\text{Nd}/^{144}\text{Nd}$  variation.

### Calculation of mantle differentiation age using combined $^{142}\text{Nd}$ and $^{143}\text{Nd}$ isotopic compositions.

The relevant decay equations for a two-stage model of mantle evolution for  $^{147}\text{Sm}$ - $^{143}\text{Nd}$  decay and  $^{146}\text{Sm}$ - $^{142}\text{Nd}$  decay are:

(Equation S1).

$$\left[ \frac{^{143}\text{Nd}}{^{144}\text{Nd}} \right]_{t_2}^{\text{mantle}} = \left[ \frac{^{143}\text{Nd}}{^{144}\text{Nd}} \right]_{\text{present}}^{\text{CHUR}} + \left[ \frac{^{147}\text{Sm}}{^{144}\text{Nd}} \right]_{\text{present}}^{\text{CHUR}} \times (1 - e^{-\lambda_{147}t_1}) + \left[ \frac{^{147}\text{Sm}}{^{144}\text{Nd}} \right]_{\text{present}}^{\text{mantle}} \times (e^{-\lambda_{147}t_1} - e^{-\lambda_{147}t_2})$$

And, (Equation S2)

$$\left[ \frac{^{142}\text{Nd}}{^{144}\text{Nd}} \right]_{t_2}^{\text{mantle}} = \left[ \frac{^{142}\text{Nd}}{^{144}\text{Nd}} \right]_{\text{present}}^{\text{CHUR}} - \left[ \frac{^{146}\text{Sm}}{^{144}\text{Sm}} \right]_{T_0}^{\text{CHUR}} \\ \times \left[ \frac{^{144}\text{Sm}}{^{147}\text{Sm}} \right]_{\text{present}}^{\text{CHUR}} \times \left[ \frac{^{147}\text{Sm}}{^{144}\text{Nd}} \right]_{\text{present}}^{\text{CHUR}} \times \left( e^{-\lambda_{146}(T_0-t_1)} \right) + \left[ \frac{^{147}\text{Sm}}{^{144}\text{Nd}} \right]_{t_1}^{\text{mantle}} \times \left( e^{-\lambda_{146}(T_0-t_2)} - e^{-\lambda_{146}(T_0-t_1)} \right)$$

where  $T_0=4.567$  Ga, the age of beginning of Earth accretion,  $t_1$ =time of formation of depleted (high Sm/Nd) mantle source, and  $t_2$ = timing of sampling of this depleted source, in this case the crystallization age of the rock being analysed. CHUR (=bulk silicate Earth) compositions used are  $^{143}\text{Nd}/^{144}\text{Nd}=0.512638$  and  $^{147}\text{Sm}/^{144}\text{Nd}=0.1966$ ; initial  $^{146}\text{Sm}/^{144}\text{Sm}=0.0075\pm 0.0025$  (S4). Decay constants: For  $\lambda_{147} = 6.54 \times 10^{-12}\text{yr}^{-1}$  and  $\lambda_{146} = 6.74 \times 10^{-9}\text{yr}^{-1}$ .

## References

- S1. V. Bennett, A. Nutman, M. McCulloch, *Earth Planet. Sci. Lett.* **119**, 299 (1993).  
 S2. M. Rehkamper, M. Gartner, S. J. G. Galer, S. L. Goldstein, *Chem. Geol.* **129** 201 (1996).  
 S3. G. Caro, B. Bourdon, J.-L. Birck, S. Moorbath, *Geochim. Cosmochim. Acta* **70** 164 (2006).  
 S4. Y. Amelin, A. Ghosh, E. Rotenberg, *Geochim. Cosmochim. Acta* **69**, 505 (2005).  
 S5. A. Nutman, V. Bennett, C. Friend, K. Horie, H. Hidaka, *Contrib. Mineral. Petrol.* **354** 385 (2007).  
 S6. A. Nutman et al., *Precambrian Res.* **117**, 185 (2002).  
 S7. H. Baadsgaard, A. Nutman and D. Bridgwater, *Geochim. Cosmochim. Acta* **50**, 2171 (1986).  
 S8. F. Jenner, Australian National University Ph.D. thesis, 275pp. (2007).  
 S9. J. Crowley, *Precamb. Res.* **126**, 235 (2003).  
 S10. A. Nutman, V. Bennett, C. Friend and M. Norman, *Contrib. Mineral. Petrol.* **137**, 364 (1999).  
 S11. M. Honda, A. Nutman and V. Bennett *Earth Planet. Sci. Lett.* **207**, 69 (2003).  
 S12. S. Moorbath, M. Whitehouse, B. Kamber, *Chemical Geology* **135**, 213 (1997).  
 S13. A. Gancarz, G. Wasserburg, *Geochim. Cosmochim. Acta* **41**, 1283 (1977).  
 S14. A. Nutman, P. Kinny, W. Compston, I.S. Williams, *Precambrian Research*, **52**, 275 (1991).  
 S15. A. Nutman, V. Bennett, P. Kinny, R. Price, *Tectonics* **12**, 971 (1993).  
 S16. G. Caro, B. Bourdon, J.-L. Birck, S. Moorbath *Geochim. Cosmochim. Acta* **70**, 164 (2006).  
 S17. M. Boyet et al., *Earth Planet. Sci. Lett.* **214**, 447 (2003).  
 S18. M. Boyet, R. Carlson, *Earth Planet. Sci. Lett.* **250**, 254 (2006).

**Table S1. Sample localities and references to detailed descriptions and age information**

Sample No.	General locality	Rock type	Age (Ma)	Notes
<b>Southwest Greenland samples</b>				
G01/113	island south of Nuuk	homogeneous tonalite	3849±6	Locality information, SHRIMP U-Pb zircon age data, <sup>143</sup> Nd isotopic data and major and trace element geochemistry for this sample in (S5)
G99/22	island south of Nuuk	foliated tonalite	3862±16	Locality information, SHRIMP U-Pb zircon age data, <sup>143</sup> Nd isotopic data and major and trace element geochemistry for this sample in (S6)
G93/07	island south of Nuuk	homogeneous tonalite	3852±12	Locality information, SHRIMP U-Pb zircon age data, <sup>143</sup> Nd isotopic data and major and trace element geochemistry for this sample in (S5)
G01/36	Itilleq fjord	foliated tonalite	3849±6	SHRIMP U-Pb zircon age data for this sample in (S5). Sample collected from the Central gneiss unit of the Isua supracrustal belt. Published age and Sm-Nd data from this same unit (S7) are in agreement with new data presented in Table S2.
G06/3.7	Isua region	homogenous granodiorite	3698±8	Locality and major and trace element geochemistry for this sample in (S8). Minimum age of 3800 Ma is constrained by zircon U-Pb dating of an intrusive tonalite (S9). Sm-Nd data in Table S2.
JG03/52	Isua supracrustal belt	pillow basalt	>3803±3	Locality and major and trace element geochemistry for this sample in (S8). Minimum age of 3800 Ma is constrained by zircon U-Pb dating of an intrusive tonalite (S9). Sm-Nd data in Table S2.
JG03/48	Isua supracrustal belt	pillow basalt	>3803±3	Locality and major and trace element geochemistry for this sample in (S8). Minimum age of 3800 Ma is constrained by zircon U-Pb dating of an intrusive tonalite (S9). Sm-Nd data in Table S2.
G97/98	Isua region	homogeneous tonalite	3795±3	Locality, major and trace element geochemistry and U-Pb zircon age for this sample in (S10). Sm-Nd data in Table S2.
G01/91	island south of Nuuk	metagabbro	>3850	Locality and major and trace element geochemistry in (S8). The minimum age of this mafic/ultramafic sequence is from SHRIMP U-Pb dating of intrusive tonalites (S6).
JG03/11	island south of Nuuk	metavolcanic amphibolite	>3850	Locality and major and trace element geochemistry in (S8). The minimum age of this mafic/ultramafic sequence is from SHRIMP U-Pb dating of intrusive tonalites (S6). Sm-Nd data in Table S2.
JG03/12	island south of Nuuk	metavolcanic amphibolite	>3850	Locality and major and trace element geochemistry in (S8). The minimum age of this mafic/ultramafic sequence is from SHRIMP U-Pb dating of intrusive tonalites (S6). Sm-Nd data in Table S2.
JG03/36	island south of Nuuk	metavolcanic amphibolite	>3850	Locality and major and trace element geochemistry in (S8). The minimum age of this mafic/ultramafic sequence is from SHRIMP U-Pb dating of intrusive tonalites (S6). Sm-Nd data in Table S2.
G97/112	peninsula south of Nuuk	ferrodiorite	3640±11	U-Pb zircon age is from (S11). Sm-Nd isotopic data for the unit in (S12).
G97/111	peninsula south of Nuuk	granite-augen gneiss	3642±3	Sample collected from blast site of Gancarz and Wasserburg as described in their Pb isotopic study (S13). U-Pb zircon age of the unit is from (S11). Sm-Nd isotopic data for the unit in (S12).
<b>Western Australian samples</b>				
88/28	Narryer Gneiss Complex	foliated tonalite	3731±4	Tonalite gneiss south of the Jack Hills. Locality and U-Pb SHRIMP zircon age of this sample in (S14). Sm-Nd data for this sample in (S15)
88/173	Narryer Gneiss Complex	foliated tonalite	3730±5	Gneiss unit approx. 10km south of the Jack Hills. Locality and U-Pb SHRIMP zircon age of this sample in (S15). Sm-Nd data for this sample in (S15).

**Table S2. Sm and Nd concentrations and isotopic data**

Sample	Age (Ga) <sup>a</sup>	Nd ug/g <sup>b</sup>	Sm ug/g	<sup>147</sup> Sm/ <sup>144</sup> Nd	<sup>143</sup> Nd/ <sup>144</sup> Nd(0) <sup>c</sup>	$\pm 2 \sigma^d$	$\epsilon_{Nd}(0)^e$	<sup>143</sup> Nd/ <sup>144</sup> Nd(t)	$\epsilon_{Nd}(t)^e$	ref.
G01/113	3849±6	8.7088	1.4393	0.0999	0.510328	0.000009	-45.06	0.50778	3.1	S5
G93/07	3852±12	15.6972	2.9779	0.1146	0.510704	0.000008	-37.73	0.50778	3.2	S5
G99/22	3862±16	39.9960	7.6456	0.1155	0.510745	0.000008	-36.93	0.50780	3.5	S5
JG03/11	>3850	5.3481	1.8894	0.2137	0.513254	0.000006	12.02	0.50781	3.6	this study
JG03/12	>3850	3.0235	0.9638	0.1927	0.512724	0.000006	1.68	0.50781	3.7	this study
JG03/36	>3850	4.4247	0.9430	0.1288	0.511022	0.000008	-31.52	0.50774	2.3	this study
G06/3.7	3698±8	22.6290	3.2093	0.0857	0.509980	0.000006	-51.85	0.50788	1.2	this study
JG03/52	>3803±3	4.6416	1.4078	0.1834	0.512293	0.000007	-6.73	0.50768	-0.2	this study
JG03/48	>3803±3	3.1708	0.6466	0.1233	0.511013	0.000008	-31.70	0.50791	4.2	this study
G97/98	3795±3	18.1674	2.9594	0.0984	0.510287	0.000007	-45.86	0.50782	2.3	this study

Table notes: a) crystallization age of sample (Table S1). b) concentration in ug/g.

c) measured <sup>143</sup>Nd/<sup>144</sup>Nd ratio. d) internal precision =  $\pm 2\sigma/n$ , where n is number of measurement cycles.

e)  $\epsilon^{143}Nd(t) = [(^{143}Nd/^{144}Nd(t)_{sample}/^{143}Nd/^{144}Nd(t)_{CHUR}) - 1] \times 10^4$ , where t refers to the crystallization age of the sample and CHUR is the chondritic reservoir composition used to represent bulk silicate Earth with present day <sup>143</sup>Nd/<sup>144</sup>Nd = 0.512638 and <sup>147</sup>Sm/<sup>144</sup>Nd = 0.1966.  $\epsilon^{143}Nd(O)$  is the present day composition relative to CHUR.

f) measured <sup>143</sup>Nd/<sup>144</sup>Nd ratio corrected for in situ decay based on the age of the sample and the measured <sup>147</sup>Sm/<sup>144</sup>Nd. Precision of initial compositions is  $\leq 0.5$  epsilon units.





Figure S1.

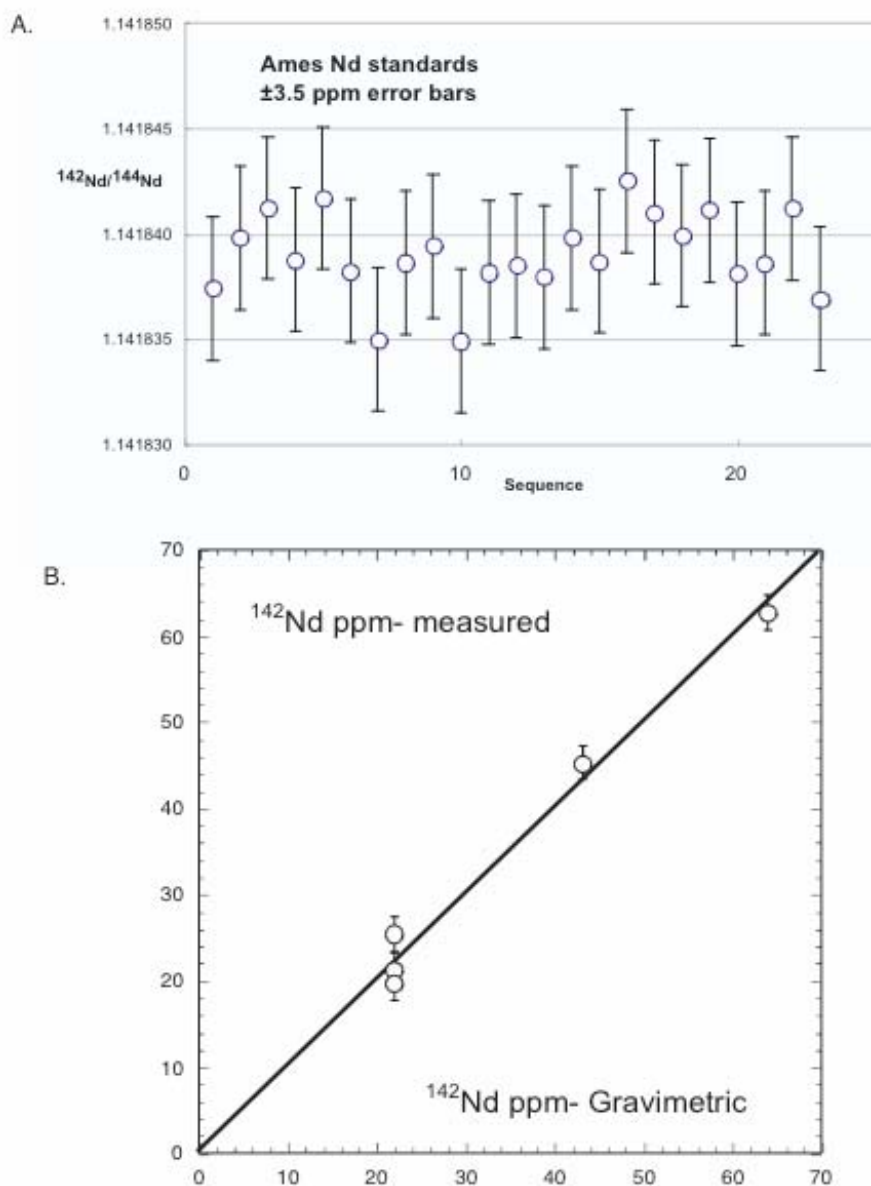


Figure S1. A. Long-term reproducibility of AMES standard for  $^{142}\text{Nd}/^{144}\text{Nd}$  as measured on the JSC TRITON TIMS. Errors bars reflect  $2\sigma$  external reproducibility of  $\pm 3.5$  ppm over 6 month period. B. Comparison between measured and known compositions of gravimetrically prepared  $^{142}\text{Nd}$  enriched solutions, demonstrating the ability to accurately determine  $^{142}\text{Nd}$  variations over a wide compositional range.

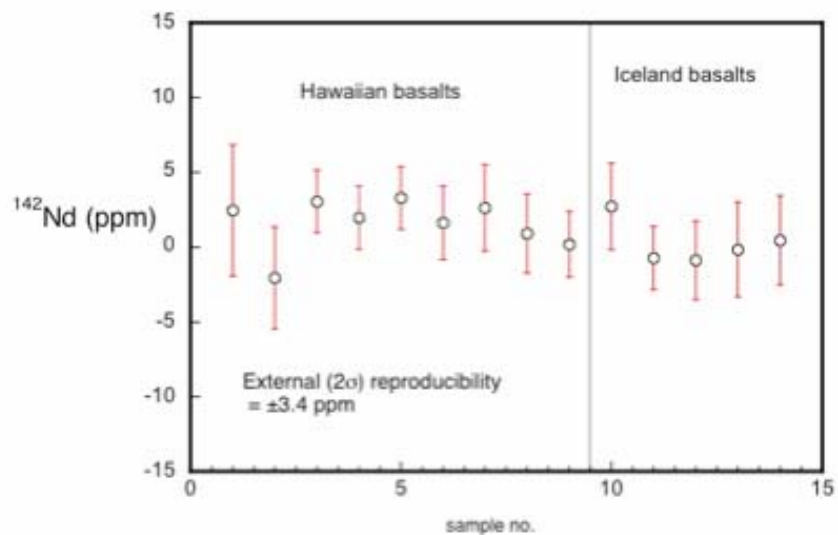


Figure S2.  $^{142}\text{Nd}/^{144}\text{Nd}$  compositions presented as ppm differences from the modern terrestrial reference. All data were measured at the JSC/NASA lab using identical chemical processing and measurement protocols as used for the Archean samples. Sample error bars are  $\pm 2$  S.E. The  $^{142}\text{Nd}$  (ppm) of these 14 rocks is  $1.1 \pm 3.4$  ppm ( $2\sigma$  external reproducibility).

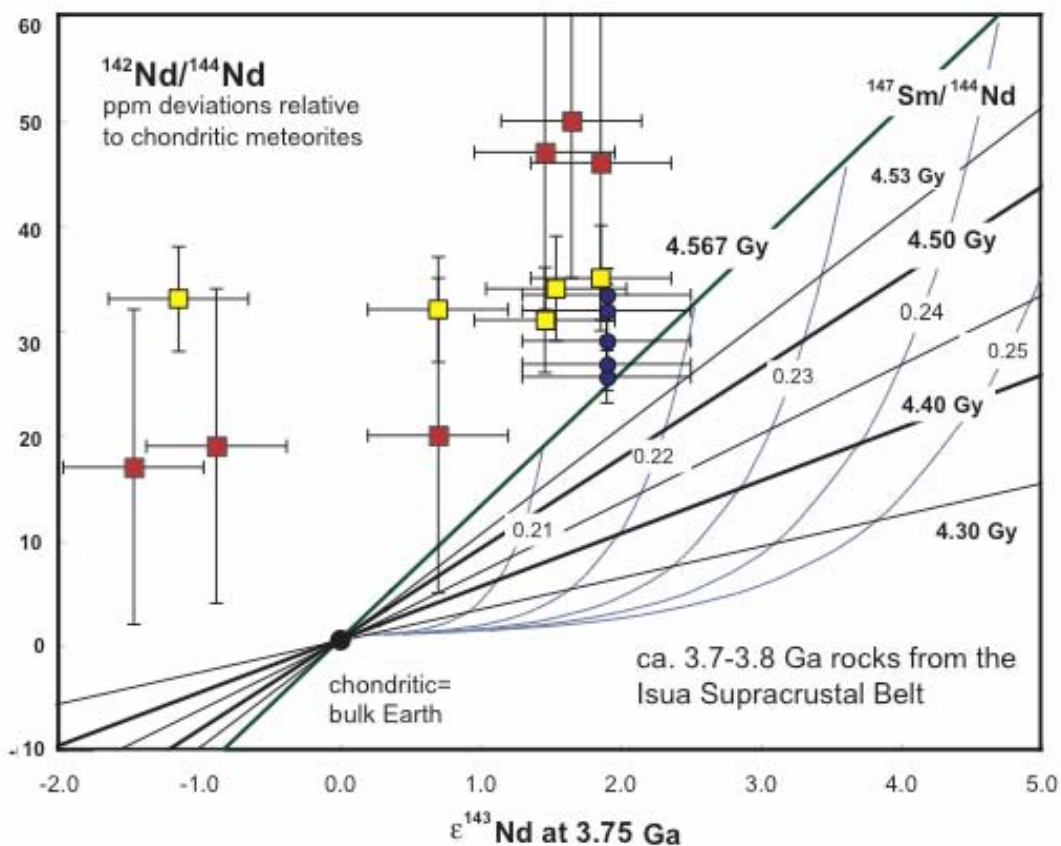


Figure S3. Two-stage model of  $^{142}\text{Nd}$ - $^{143}\text{Nd}$  isotopic evolution (see Fig. 1 caption, equations *S1*, *S2*). Shown here are calculated isotopic compositions at 3.75 Ga. Plotted are published data for 3.7-3.8 Ga rocks from the Isua Supracrustal Belt. For every sample the data are as given in the original publications. Blue circles are metasediments from Caro et al., (*S16*) which were all assigned an initial (3.74 Ga)  $\epsilon^{143}\text{Nd}$  of  $+1.9 \pm 0.6$  based on regional whole rock isochron data. Red squares are Isua metabasalts from Boyet et al., (*S17*), with given ages of 3.78 Ga. Yellow squares are additional  $^{142}\text{Nd}$  data (*S18*) for previously analysed metabasalts (*S17*) with the  $^{143}\text{Nd}$  data for these samples from *S17*. Many of the samples lie to the left of all possible compositions generated using 2-stage models, requiring a more complex petrogenetic history for these rocks.